IEEE Access
Multidisciplinary | Rapid Review | Open Access Journal

Received October 20, 2021, accepted November 22, 2021, date of publication November 29, 2021,
date of current version December 7, 2021.

Digital Object Identifier 10.1109/ACCESS.2021.3131169

Wireless Information and Power Transfer Using Full-Duplex Self-Energy Recycling Relays

JIAMAN LI, LE CHUNG TRAN, (Senior Member, IEEE), AND FARZAD SAFAEI, (Senior Member, IEEE)
School of Electrical, Computer and Telecommunications Engineering, University of Wollongong (UOW), Wollongong, NSW 2522, Australia
Corresponding author: Jiaman Li (jl797@uowmail.edu.au)

ABSTRACT This paper proposes a Polarization-Enabled Digital Self-Interference Cancellation (PDC)-based Full-Duplex (FD) network with an energy-harvesting-enabled source and a Self-Energy Recycling (SER)-enabled relay. The fixed power supply at the relay is only used in the first phase to broadcast energy signals to the source. During this process, the receive antenna of the relay also receives the energy signals, allowing the relay to recycle its own energy. In the remaining phase, the recycled power is used at the relay to forward signals from the source to the destination, using the PDC-based full-duplex technique. An in-depth analysis and comparison of the throughput of the proposed system with that of the non-recycling counterpart are presented. The power saving and throughput improvement capabilities of the SER enabled system is researched. In particular, the consumed power in the proposed system can be reduced by up to 80% to achieve the same throughput compared to the non-recycling system for a small-to-medium distance range between the relay and the destination. Alternatively, the proposed FD-SER system can boost the system throughput by 1.61 times the non-recycling counterpart with the same power consumption.

INDEX TERMS Self-energy recycling, full-duplex, self-interference, RF-powered relay channel.

I. INTRODUCTION

The Energy Harvesting (EH) technology has become increasingly attractive as an appealing solution to provide long-lasting power for energy-constrained wireless sensor networks. Different from absorbing energy from the intermittent and unpredictable natural resources, such as solar, wind, and vibration, harvesting energy from the Radio Frequency (RF) signal radiated by ambient transmitters has received tremendous attentions. The RF signal can convey both information and energy at the same time, which facilitates the development of Simultaneous Wireless Information and Power Transfer (SWIPT). Besides, ambient RF is widely available from base stations, WIFI hot spots, and mobile phones in the current information era. The RF approach is cost-effective for communication networks as peripheral equipment needed to utilize external energy sources can be avoided.

Relaying and Full-Duplex (FD) techniques have gained considerable attraction from researchers for their ability to improve system throughput. Besides, the demand for low-labor-cost and long-lifetime wireless communication systems has been increasing in recent years. Thus, the FD relaying system with wireless power transfer has also attracted the attention of many scholars. However, the main challenge for the FD transmission is to deal with the Self-Interference (SI) signal. SI signals can be suppressed by Self-Interference Cancellation (SIC) methods. The three main types of SIC methods are passive cancellations, digital cancellations, and analog cancellations, which can be applied jointly to maximize the SI suppression [1]. The FD EH relaying systems are studied in [2], [3] to increase system spectral efficiency, where SIC methods are applied to suppress SI signals. Alternatively, SI signals can also be utilized in a Self-Energy Recycling (SER) process [4]–[16] to improve the energy efficiency. The literature comparison of wireless power transfer-aided SER relaying systems is illustrated in Table 1. More specifically, in [4], a buffer-aided Half-Duplex (HD) wireless-powered SER relay system with two antennas at the relay and one antenna at the source and destination is considered. A fixed-antenna assignment and an adaptive-antenna assignment are proposed to improve the system throughput. The authors in [5]–[12] consider two-phase SWIPT systems with SER at the relay node.

The associate editor coordinating the review of this manuscript and approving it for publication was Francisco Rafael Marques Lima.

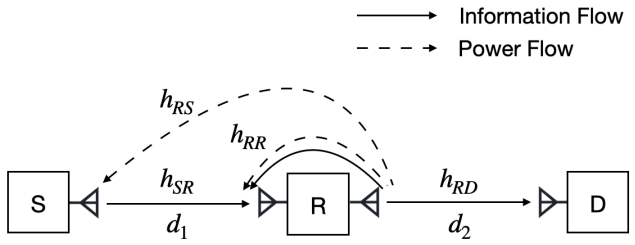

FIGURE 1. Schematic of the proposed FD-SER system.

With T representing the total block duration, the first phase of the duration $T/2$ is used by the source for sending information to the relay. The second phase of the remaining time $T/2$ is used by the relay for receiving energy signals from the source, and concurrently, transmitting information to the destination. Particularly, a portion of its own transmit signal can be harvested and reused by the relay via the loopback channel. The SI signal at the relay is in fact beneficial since the relay not only harvests energy from the source, but also recycles energy from the self-interfering link. In all these time-switching-based SWIPT relaying systems [5]–[12], the information signal is transmitted and received in different phases, so that the SIC is not required to eliminate SI. However, this also means that the relay cannot receive information from the source and transmit information to the destination at the same time, thus limiting the system throughput. In [13], [14], the SER-based decode-and-forward FD relaying networks are studied with an efficient power allocation strategy. The relay in these systems works in a FD mode and receives information from the source and its own transmitter. A portion of the received signal is used for the EH process while the remaining portion of the received signal is used for the decoding and forwarding information to the destination. However, the disadvantage of the methods proposed in [13], [14] is that the practical EH circuits cannot forward the received information and simultaneously extract power from the same received signal [17]. In [15], the authors consider a FD relaying system with multiple transmit and receive antennas at the relay. The proposed antenna allocation scheme can allot the antennas at both transmit and receive ends for either SER or information relaying. The spectral efficiency and energy efficiency are improved at the cost of a complicated antenna allocation technique. In [16], the authors study a power-splitting based amplify-and-forward FD system, where the signal transmission and reception and SER are performed in one phase. However, there are no specific SIC schemes mentioned in [13]–[16].

II. MOTIVATION AND CONTRIBUTION

Inspired by the recent studies in the SER, we propose a full-duplex self-energy recycling relaying system with EH capabilities at both the source node and the relay node. For brevity, the proposed system is named as the FD-SER system here. The source and destination are equipped with a single antenna, while the relay has two antennas to facilitate FD transmission. The proposed two-phase time-splitting protocol lets the source and relay harvest energy in the first phase from the energy signal, which is broadcast from the relay powered by a fixed power supply. A portion of the energy of the transmitted signals is recycled at the relay via the SI channel. In the second phase, the relay receives information from the source and simultaneously transmits information to the destination. The transmission of the source and relay depends solely on the harvested energy. The SI signal in this phase is canceled by a Polarization-Enabled Digital Self-Interference Cancellation (PDC) scheme. The proposed system suits the wireless sensor networks, such as the body sensor networks [18] and the military sensor networks. For example, an energy-constrained sensor is placed within the human body or underground so that replacing the battery to prolong its lifetime is inconvenient. Instead, this sensor can harvest energy from the nearby relay. The relay node also can assist the source sensor to forward information to the destination when direct communication is not possible. The SER is enabled at the relay, which improves the system energy and power efficiencies as proved later in this paper. The proposed FD-SER system will be compared with the FD non-energy-recycling EH relaying system with wireless power transfer from the relay to the source proposed in [19]. For brevity, the non-recycling system is named as the FD-NER system, which is comprised of an EH source, a relay, and a destination. In [19], the relay uses a fixed power supply in the whole transmission process since the relay does not have the self-recycling capability. Thus, no loop-back SER channel nor SER power is considered in the FD-NER system in [19]. The differences of the system model and analytical expressions between this paper and [19] will be elaborated in Section VI. The impact of the EH fraction, transmit Signal-to-Noise (SNR) ratio, and Source-Relay (S-R) distances and Relay-Destination (R-D) distances on the system throughput in both systems are then examined in this paper.

The major contributions of this work are summarized as follows.

1) In this paper, a PDC-based FD-SER system is proposed. We have proved that the throughput of the proposed system is comparable with the throughput of the FD-NER system in a small-to-medium R-D distance range while the total power consumption is significantly reduced.
2) The relation between the normalized power consumption and the normalized throughput has been investigated. It has been shown that the proposed recycling system can save up to 80% of the total consumed power while achieving almost the same throughput as the FD-NER one. Alternatively, with the same total power, the relay in our proposed FD-SER system can use a higher power to broadcast energy to the source

TABLE 1. The literature comparison of wireless power transfer-aided SER relaying systems, where (√) represents Yes, (×) represents No, (–) represents SIC Schemes are not applicable, and (＼) represents No specific scheme is mentioned.

	No. of nodes	Assumption of direct link from S to D	Energy harvesting at S	Energy harvesting at R	Self-energy Recycling at R	Antennas	Protocol	Simultaneous transmission and reception of information at R	Active SIC scheme
[4]	4	√	×	√	√	Single at S and D; Two at R	Decode-and-Forward;	×	–
[5]	3	×	×	√	√	Multiple-Input Single-Output	Amplify-and-Forward;	×	–
[6]	3	×	×	√	√	Multiple at S and R; Single at D	Amplify-and-Forward;	×	–
[7]	3	×	×	√	√	Single at S and D; Two at R	Amplify-and-Forward;	×	–
[8]	3	×	×	√	√	Multiple at S and R; Single at D	Amplify-and-Forward;	×	–
[9]	4	×	×	√	√	Multiple at S and R; Single at D	Amplify-and-Forward;	×	–
[10]	3	√	×	√	√	Single at S and D; Two at R	Amplify-and-Forward; Decode-and-Forward; Quantize-Map-Forward;	×	–
[11]	3	×	×	√	√	Multiple at S, R, and D	Amplify-and-Forward;	×	–
[12]	3	×	×	√	√	Single at S and D; Two at R	Decode-and-Forward;	×	–
[13]	3	×	×	√	√	Multiple at S and R; Single at D	Decode-and-Forward	√	＼
[14]	3	×	×	√	√	Single at S and D; Two at R	Decode-and-Forward;	√	＼
[15]	3	×	×	√	√	Multiple at R; Single at S and D	Decode-and-Forward	√	＼
[16]	3	×	×	√	√	Multiple at S and R; Single at D	Amplify-and-Forward	√	＼
This paper	3	×	√	√	√	Dual-polarized antennas; Single at S and D; Two at R	Amplify-and-Forward	√	√

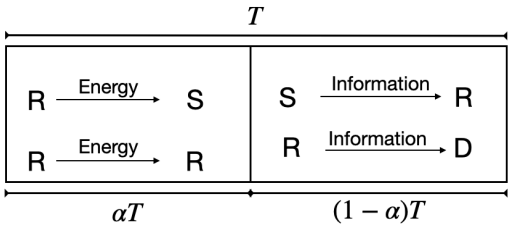

FIGURE 2. Illustration for the proposed two-phase protocol.

(and to itself) in the first phase, compared to the FD-NER one, since the FD-SER system only uses the harvested power to forward the signals from the source to the destination in the remaining time. The throughput of the proposed system is revealed to be boosted by 1.61 times that of the FD-NER system.

3) The trade-off between the proposed system and the FD-NER one, with the same total power consumption, is examined. It is shown that the proposed system is very promising as it outperforms the FD-NER one in most cases.

The rest of this paper is organized as follows. Section III provides an overview of the system model and transmission protocol. Section IV models the transmission of the energy signal and the information signal in one block time. The analytical expressions for the proposed FD-SER system and the FD-NER system are derived in Section V. Section VI presents the simulation results and Section VII concludes the paper.

III. SYSTEM MODEL

In this paper, we consider an amplify-and-forward FD information transmission system with an EH source (S), a hybrid power-supplied-and-SER relay (R), and a destination (D) as shown in Fig. 1. S and D are equipped with one dual-polarized antenna each while R is equipped with two sets of dual-polarized antennas, i.e., one for transmission and the other for reception. The direct link between S and D is assumed to be unavailable due to, for example, heavy shadowing effects. Denote h_{SR}, h_{RS}, h_{RR}, and h_{RD} as the channel coefficients of the Rayleigh block fading channels between S and R; R and S; the transmit (Tx) and receive (Rx) antennas at R; and R and D, respectively. We assume their expectation values satisfy $E\{|h_{SR}|^2\} = E\{|h_{RS}|^2\} = E\{|h_{RR}|^2\} = E\{|h_{RD}|^2\} = 1$, where $E\{.\}$ denotes the expectation operation. Denote d_1 and d_2 as the distances between S $\rightarrow$ R and between R $\rightarrow$ D. Denote d_3 as the distance between the Tx and Rx antennas of the relay. The two-phase protocol used in our system is illustrated in Fig. 2. The total duration of one block is T. The first and second phases, namely the energy harvesting phase and the information transmission phase, occupy the duration αT and $(1-\alpha)T$, respectively, where $0 < \alpha < 1$. The following section analyzes the transmission process of energy and information signals.

IV. SIGNAL MODEL

A. ENERGY HARVESTING PHASE

During the energy harvesting phase, the antenna at S works in the receiving mode. R works in a HD mode and uses its fixed power supply P_r to broadcast the energy signal. S and R are equipped with linear EH modules. Thus, not only S harvests the energy from R, but also the EH circuitry at R recycles a portion of its own transmitted energy via a loop channel h_{RR}. The polarization of the Tx antenna at R matches the polarization of the Rx antennas at S and R for an optimal reception. The harvested power at S and R will be used for the information transmission in the next phase.

The received energy signal at the source node S is

$$y_s = \sqrt{\frac{P_r}{d_1^\beta}} h_{RS} x_e + n_s, \tag{1}$$

where P_r is the fixed power supply at R, which is only used in the first phase as the energy source, d_1 is the distance from the source to the relay, β is the path loss exponent, h_{RS} is the channel coefficient of the $R \rightarrow S$ channel, x_e is the energy symbol with $E\{|x_e|^2\} = 1$, and n_s is the Additive White Gaussian Noise (AWGN) at S with a variance of N_0.

Using (1), the total received RF energy E_s of the source node during the time αT is

$$E_s = \frac{\eta_1 P_r |h_{RS}|^2}{d_1^\beta} \alpha T, \tag{2}$$

where $0 < \eta_1 < 1$ is the energy conversion efficiency of the source node. Thus, the average RF power for transmission during the next phase at the source is given by

$$P_s = \frac{E_s}{(1-\alpha)T} = \frac{\eta_1 \alpha P_r |h_{RS}|^2}{(1-\alpha) d_1^\beta}. \tag{3}$$

In addition, the received energy signal at the relay node R from its own transmitter is

$$y_{er} = \sqrt{\frac{P_r}{d_3^\beta}} h_{RR} x_e + n_r, \tag{4}$$

where n_r is the AWGN at R with power N_0. The self-recycling power which will be used to transmit information in the next phase at the relay is

$$P_{er} = \frac{\eta_2 \alpha P_r |h_{RR}|^2}{(1-\alpha) d_3^\beta}, \tag{5}$$

where $0 < \eta_2 < 1$ is the energy conversion efficiency of the relay node. Generally, the system is appropriate for any values of $\eta_1, \eta_2 \in (0, 1)$. In practice, we assume $\eta_2 > \eta_1$ since the receiver at R is closer to its own transmitter than the receiver at S, thus having a larger input power into the EH circuit [20], [21]. The harvested power P_s and P_{er} will be used in the second phase for information transmission as there is no fixed power supply at S and R in the information transmission phase.

B. INFORMATION TRANSMISSION PHASE

In this phase, the antenna at S works in the transmitting mode. The source uses the harvested power P_s to transmit the information signal to the relay. The relay works in the FD mode to receive information and forward information at the same time on the same frequency. The power used by the relay to forward information is the recycled power P_{er}. The power supply P_r is switched off in this phase for saving energy. The polarization of the antenna at S and the antennas at R is different from the first phase. Specifically, the polarization of the Rx antenna at R matches that of the Tx antenna at S but differs from that of the Tx antenna at R. The aim is that R receives the maximum power of the desired information signal from S while receiving the minimum amount of the SI power from its own transmitter. Denote the polarization state of the desired information signal as $\mathbf{S}$ and the polarization state of the SI signal as $\mathbf{I}$. $\mathbf{S}$ and $\mathbf{I}$ are given as below

$$\begin{aligned}\mathbf{S} &= \left[\cos(\varepsilon_s) \quad \sin(\varepsilon_s)\exp(j\delta_s)\right]^{\mathrm{T}},\\ \mathbf{I} &= \left[\cos(\varepsilon_i) \quad \sin(\varepsilon_i)\exp(j\delta_i)\right]^{\mathrm{T}}.\end{aligned} \tag{6}$$

where $\varepsilon_i, \varepsilon_s \in [0, \pi/2]$ are polarized angles of the dual-polarized antennas, $\delta_i, \delta_s \in [0, 2\pi]$ are phase differences between the vertical and horizontal polarized components of the dual-polarized antennas, and $(.)^{\mathrm{T}}$ represents the transpose of a vector or matrix. $\mathbf{S}$ and $\mathbf{I}$ are unit vectors, i.e., $\mathbf{S}^{\mathrm{H}}\mathbf{S} = \mathbf{I}^{\mathrm{H}}\mathbf{I} = 1$ and $\mathbf{S} \neq \mathbf{I}$. The received signal at R is

$$\mathbf{y}_r = \sqrt{\frac{P_s}{d_1^{\beta}}}h_{SR}\mathbf{S}x_s + \sqrt{\frac{P_{er}}{d_3^{\beta}}}h_{RR}\mathbf{I}x_r + \mathbf{N}_r, \tag{7}$$

where x_r is the loop-back interference signal, i.e., a delayed version of $\hat{y}_r$ which will be mentioned later in (17), and $E\{|x_r|^2\} = 1$. h_{RR} is the SI channel of the relay. The AWGN at R is $\mathbf{N}_r = \begin{bmatrix}\mathrm{n}_H \\ \mathrm{n}_V\end{bmatrix}$, where n_H represents the horizontal polarized component and n_V represents the vertical polarized component. n_H and n_V obey the Gaussian distribution with a zero mean and a variance of $\frac{N_0}{2}$.

The desired received signal in $\mathbf{y}_r$ is interfered by the SI signal x_r. The signal x_r can be canceled by the PDC scheme utilizing the polarization states $\mathbf{S}$ and $\mathbf{I}$ and the oblique projection $\mathbf{Q}_{\mathrm{SI}}$. To explain the oblique projections, we first introduce the orthogonal projections. An orthogonal projection has a null space that is orthogonal to its range [22]. For an orthogonal projection $\mathbf{P}_{\mathrm{S}}$ whose range is $\langle\mathbf{S}\rangle$ and null space is $\langle\mathbf{I}\rangle = \langle\mathbf{S}\rangle^{\perp}$, we have

$$\begin{aligned}\mathbf{P}_{\mathrm{S}}\mathbf{S} &= \mathbf{S},\\ \mathbf{P}_{\mathrm{S}}\mathbf{I} &= \mathbf{0},\end{aligned} \tag{8}$$

where $\mathbf{0}$ is a zero vector, i.e., $\mathbf{0} = \begin{bmatrix}0 & 0\end{bmatrix}^{\mathrm{T}}$.

The well-known formulas to build orthogonal projections with the range $\langle\mathbf{S}\rangle$ and $\langle\mathbf{I}\rangle$, respectively, are given by

$$\begin{aligned}\mathbf{P}_{\mathrm{S}} &= \mathbf{S}(\mathbf{S}^{\mathrm{H}}\mathbf{S})^{-1}\mathbf{S}^{\mathrm{H}},\\ \mathbf{P}_{\mathrm{I}} &= \mathbf{I}(\mathbf{I}^{\mathrm{H}}\mathbf{I})^{-1}\mathbf{I}^{\mathrm{H}},\end{aligned} \tag{9}$$

where $(.)^{\mathrm{H}}$ is the Hermitian transposition of a complex vector or matrix, and $(.)^{-1}$ is the matrix inversion. $\mathbf{P}_{\mathrm{S}}$ is called the projector onto $\langle\mathbf{S}\rangle$. The orthogonal projection with the range $\langle\mathbf{S}\rangle^{\perp}$ is

$$\begin{aligned}\mathbf{P}_{\mathrm{S}}^{\perp} &= \mathbf{E} - \mathbf{P}_{\mathrm{S}}\\ &= \mathbf{E} - \mathbf{S}\mathbf{S}^{\mathrm{H}},\end{aligned} \tag{10}$$

where

$$\mathbf{E} = \begin{bmatrix}1 & 0\\ 0 & 1\end{bmatrix}. \tag{11}$$

Based on (9), the orthogonal projection onto the linear subspace $\langle\mathbf{S}\ \mathbf{I}\rangle$ is

$$\mathbf{P}_{\mathrm{SI}} = \begin{bmatrix}\mathbf{S} & \mathbf{I}\end{bmatrix}\begin{bmatrix}\mathbf{S}^{\mathrm{H}}\mathbf{S} & \mathbf{S}^{\mathrm{H}}\mathbf{I}\\ \mathbf{I}^{\mathrm{H}}\mathbf{S} & \mathbf{I}^{\mathrm{H}}\mathbf{I}\end{bmatrix}^{-1}\begin{bmatrix}\mathbf{S}^{\mathrm{H}}\\ \mathbf{I}^{\mathrm{H}}\end{bmatrix}. \tag{12}$$

In contrast, the projection matrices of oblique projections are not orthogonal. For an oblique projection $\mathbf{Q}_{\mathrm{SI}}$ whose range is $\langle\mathbf{S}\rangle$ and null space is $\langle\mathbf{I}\rangle$, we have

$$\begin{aligned}\mathbf{Q}_{\mathrm{SI}}\mathbf{S} &= \mathbf{S},\\ \mathbf{Q}_{\mathrm{SI}}\mathbf{I} &= \mathbf{0}.\end{aligned} \tag{13}$$

The oblique projection can be built by decomposing the orthogonal projection $\mathbf{P}_{\mathrm{SI}}$, i.e.,

$$\mathbf{P}_{\mathrm{SI}} = \mathbf{Q}_{\mathrm{SI}} + \mathbf{Q}_{\mathrm{IS}}, \tag{14}$$

where

$$\begin{aligned}\mathbf{Q}_{\mathrm{SI}} &= \begin{bmatrix}\mathbf{S} & \mathbf{0}\end{bmatrix}\begin{bmatrix}\mathbf{S}^{\mathrm{H}}\mathbf{S} & \mathbf{S}^{\mathrm{H}}\mathbf{I}\\ \mathbf{I}^{\mathrm{H}}\mathbf{S} & \mathbf{I}^{\mathrm{H}}\mathbf{I}\end{bmatrix}^{-1}\begin{bmatrix}\mathbf{S}^{\mathrm{H}}\\ \mathbf{I}^{\mathrm{H}}\end{bmatrix},\\ \mathbf{Q}_{\mathrm{IS}} &= \begin{bmatrix}\mathbf{0} & \mathbf{I}\end{bmatrix}\begin{bmatrix}\mathbf{S}^{\mathrm{H}}\mathbf{S} & \mathbf{S}^{\mathrm{H}}\mathbf{I}\\ \mathbf{I}^{\mathrm{H}}\mathbf{S} & \mathbf{I}^{\mathrm{H}}\mathbf{I}\end{bmatrix}^{-1}\begin{bmatrix}\mathbf{S}^{\mathrm{H}}\\ \mathbf{I}^{\mathrm{H}}\end{bmatrix}.\end{aligned} \tag{15}$$

It is easy to realize that $\mathbf{Q}_{\mathrm{SI}}$ satisfies the properties in (13). This means $\mathbf{Q}_{\mathrm{SI}}$ is the oblique projection with the respective range $\langle\mathbf{S}\rangle$ and the respective null range $\langle\mathbf{I}\rangle$. Similarly, $\mathbf{Q}_{\mathrm{IS}}$ is the oblique projection with the respective range $\langle\mathbf{I}\rangle$ and the null range $\langle\mathbf{S}\rangle$. We choose $\mathbf{Q}_{\mathrm{SI}}$ as the oblique projection of the PDC scheme in our system to preserve the desired signal while canceling the SI signal. From (15), the oblique projection with the range $\langle\mathbf{S}\rangle$ can be simplified to

$$\mathbf{Q}_{\mathrm{SI}} = \mathbf{S}\left[\mathbf{S}^{\mathrm{H}}\mathbf{P}_{\mathrm{I}}^{\perp}\mathbf{S}\right]^{-1}\mathbf{S}^{\mathrm{H}}\mathbf{P}_{\mathrm{I}}^{\perp}, \tag{16}$$

where $\mathbf{P}_{\mathrm{I}}^{\perp} = \mathbf{E} - \mathbf{P}_{\mathrm{I}} = (\mathbf{E} - \mathbf{I}\,\mathbf{I}^{\mathrm{H}})$ is the orthogonal projection with the range $\langle\mathbf{I}\rangle^{\perp}$.

The received signal at R, $\mathbf{y}_r$, is processed by the PDC scheme, which includes two main operations. Firstly, the oblique projection operator $\mathbf{Q}_{\mathrm{SI}}$ is applied to maintain the desired signal and cancel the SI signal by utilizing the property $\mathbf{Q}_{\mathrm{SI}}[\mathbf{S} \quad \mathbf{I}] = [\mathbf{S} \quad \mathbf{0}]$. Secondly, the remaining $\mathbf{S}$ in the signal part after the oblique projection will be eliminated by multiplying $\mathbf{S}^{\mathrm{H}}$, i.e., $\mathbf{S}^{\mathrm{H}}\mathbf{S} = 1$, which can de-polarize the

desired signal. Thus, the post-processed signal at the output of the PDC scheme $\hat{y}_r$ is expressed as

$$\begin{aligned}\hat{y}_r &= \mathbf{S}^{\mathrm{H}}\mathbf{Q}_{\mathrm{SI}}\left(\sqrt{\frac{P_s}{d_1^{\beta}}}h_{SR}\mathbf{S}x_s + \sqrt{\frac{P_{er}}{d_3^{\beta}}}h_{RR}\mathbf{I}x_r + \mathbf{N}_r\right)\\ &= \sqrt{\frac{P_s}{d_1^{\beta}}}h_{SR}x_s + \hat{n}_r,\end{aligned} \tag{17}$$

where $\hat{n}_r = \mathbf{S}^{\mathrm{H}}\mathbf{Q}_{\mathrm{SI}}\mathbf{N}_r$. Denote ρ as the polarization dissimilarity factor of $\mathbf{S}$ and $\mathbf{I}$. The expression of ρ can be defined as

$$\begin{aligned}\rho &= 1 - \|\mathbf{I}^{\mathrm{H}}\mathbf{S}\|^2 = 1 - \mathbf{S}^{\mathrm{H}}\mathbf{I}\mathbf{I}^{\mathrm{H}}\mathbf{S}\\ &= \mathbf{S}^{\mathrm{H}}\mathbf{P}_{\mathrm{I}}^{\perp}\mathbf{S},\end{aligned} \tag{18}$$

where $\|\cdot\|$ denotes the Euclidean norm. The power of $\hat{n}_r$ is $E\left[\|\mathbf{S}^{\mathrm{H}}\mathbf{Q}_{\mathrm{SI}}\mathbf{N}_r\|^2\right] = \frac{N_0}{2\rho}$. From (18), when the vectors $\mathbf{S}$ and $\mathbf{I}$ are orthogonal, i.e., $\mathbf{I}^{\mathrm{H}}\mathbf{S} = 0$, ρ gets the maximum value 1. The value $\rho = 0$ occurs when $\mathbf{I}^{\mathrm{H}}\mathbf{S} = 1$. However, $\mathbf{S} \neq \mathbf{I}$ leads to $\rho \neq 0$. Thus, the range of ρ is $\rho \in (0, 1]$. Eq. (17) shows that the PDC scheme can eliminate the effect of the SI channel. However, the oblique projection also causes the residual noise at the relay $\mathbf{S}^{\mathrm{H}}\mathbf{Q}_{\mathrm{SI}}\mathbf{N}_r$ with the variance $\frac{N_0}{2\rho}$. This output noise power is considered as the side-effect of the PDC scheme.

The received signal at the destination is

$$\begin{aligned}y_d &= \sqrt{\frac{\xi^2}{d_2^{\beta}}}h_{RD}\hat{y}_r + n_d\\ &= \frac{\xi h_{RD}h_{SR}\sqrt{P_s}}{\sqrt{d_1^{\beta}d_2^{\beta}}}x_s + \frac{\xi h_{RD}}{\sqrt{d_2^{\beta}}}\hat{n}_r + n_d,\end{aligned} \tag{19}$$

where $\xi^2 = \frac{P_{er}}{\frac{|h_{SR}|^2P_s}{d_1^{\beta}} + \frac{N_0}{2\rho}}$ denotes the amplifying factor at the relay in the AF protocol, and P_s and P_{er} follow Eqs. (3) and (5), respectively. It is reasonable to assume that the Rayleigh fading channels $|h_{SR}|^2$ and $|h_{RS}|^2$ are independent and identically distributed (i.i.d.) exponential random variables (RVs) with mean λ_s, $|h_{RD}|^2$ is an i.i.d. exponential RV with mean λ_d, and $|h_{RR}|^2$ is an i.i.d. exponential RV with mean λ_r.

V. THROUGHPUT ANALYSIS

In this section, the throughput of the proposed FD-SER system is analyzed. From (19), the end-to-end SNR from the source to destination is

$$\gamma_{SD} = \frac{\frac{P_s\xi^2|h_{SR}|^2|h_{RD}|^2}{d_1^{\beta}d_2^{\beta}}}{\frac{\xi^2|h_{RD}|^2N_0}{2\rho d_2^{\beta}} + N_0} = \frac{\frac{P_sP_{er}|h_{SR}|^2|h_{RD}|^2}{d_1^{\beta}d_2^{\beta}\left(\frac{|h_{SR}|^2P_s}{d_1^{\beta}} + \frac{N_0}{2\rho}\right)}}{\frac{P_{er}|h_{RD}|^2N_0}{2\rho d_2^{\beta}\left(\frac{|h_{SR}|^2P_s}{d_1^{\beta}} + \frac{N_0}{2\rho}\right)} + N_0}. \tag{20}$$

Define $X_1 \triangleq |h_{SR}|^2$, $X_2 \triangleq |h_{RS}|^2$, $Y \triangleq |h_{RD}|^2$, and $Z \triangleq |h_{RR}|^2$. From (3), (5), and (20), the SNR γ_{SD} at the destination is given by

$$\gamma_{SD} = \frac{aX_1X_2YZ}{b + cYZ + dX_1X_2}, \tag{21}$$

where

$$\begin{aligned}a &= 2P_r^2\alpha^2\eta_1\eta_2\rho,\\ b &= d_1^{2\beta}d_2^{\beta}d_3^{\beta}N_0^2(1-\alpha)^2,\\ c &= P_r\alpha\eta_2d_1^{2\beta}N_0(1-\alpha),\\ d &= 2\alpha\eta_1\rho P_rd_2^{\beta}d_3^{\beta}N_0(1-\alpha).\end{aligned} \tag{22}$$

The outage probability P_{out} is defined as the probability when the system SNR γ_{SD} is below the threshold SNR γ_{th}, where $\gamma_{th} = 2^{R_c} - 1$, and R_c is the source transmission rate in *bits/sec/Hz*.

$$\begin{aligned}P_{out} &= \Pr\{\gamma_{SD} < \gamma_{th}\}\\ &= \Pr\left\{\frac{aX_1X_2YZ}{b + cYZ + dX_1X_2} < \gamma_{th}\right\}\\ &= \Pr\left\{aX_1X_2YZ < \gamma_{th}\left(b + cYZ + dX_1X_2\right)\right\}\\ &= \Pr\left\{YZ(aX_1X_2 - \gamma_{th}c) < \gamma_{th}b + \gamma_{th}dX_1X_2\right\}.\end{aligned} \tag{23}$$

The Probability Density Function (PDF) of X_1X_2 is given by [23], [24]

$$f_{X_1X_2}(z) = \frac{2}{\lambda_s^2}K_0\left(2\sqrt{\frac{z}{\lambda_s^2}}\right), \tag{24}$$

where $K_n(x)$ is the n-th order modified Bessel function of the second kind. The Cumulative Distribution Function (CDF) of YZ is [2], [24]

$$F_{YZ}(z) = 1 - 2\sqrt{\frac{z}{\lambda_d\lambda_r}}K_1\left(2\sqrt{\frac{z}{\lambda_d\lambda_r}}\right). \tag{25}$$

From (23), the outage probability is

$$\begin{aligned}P_{out} &= \begin{cases}\Pr\left\{YZ < \frac{\gamma_{th}b + \gamma_{th}dX_1X_2}{aX_1X_2 - c\gamma_{th}}\right\}, & X_1X_2 > \frac{c\gamma_{th}}{a}\\ 1, & X_1X_2 \leqslant \frac{c\gamma_{th}}{a}\end{cases}\\ &= \int_0^{\frac{c\gamma_{th}}{a}} f_{X_1X_2}(x)dx\\ &\quad + \int_{\frac{c\gamma_{th}}{a}}^{\infty} F_{YZ}\left(\frac{\gamma_{th}b + \gamma_{th}dX_1X_2}{aX_1X_2 - c\gamma_{th}}\right)f_{X_1X_2}(x)dx.\end{aligned} \tag{26}$$

Substituting (24) and (25) into (26), we have

$$P_{out} = 1 - \frac{2}{\lambda_s^2}\int_{\frac{c\gamma_{th}}{a}}^{\infty} K_0\left(2\sqrt{\frac{x}{\lambda_s^2}}\right)uK_1(u)\,dx, \tag{27}$$

where $u = 2\sqrt{\frac{\gamma_{th}b + x\gamma_{th}d}{\lambda_d\lambda_r(ax - c\gamma_{th})}}$.

Because the information is transmitted in the duration $(1-\alpha)T$ (seconds), the system throughput can be computed as

$$\begin{aligned}R(\alpha) &= (1 - P_{out})R_c(1-\alpha)\\ &= R_c(1-\alpha)\frac{2}{\lambda_s^2}\int_{\frac{c\gamma_{th}}{a}}^{\infty} K_0\left(2\sqrt{\frac{x}{\lambda_s^2}}\right)uK_1(u)\,dx.\end{aligned} \tag{28}$$

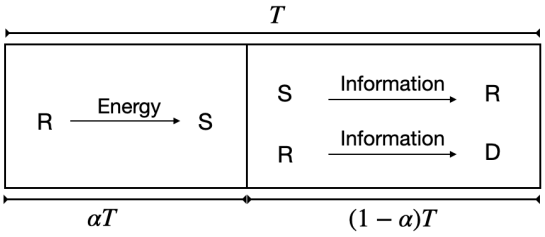

FIGURE 3. Two-phase protocol of the NER system.

Recall that R_c is the source transmission rate. The final expression of the throughput in (28) depends on the outage probability, which in turn depends on the self-recycling power at the relay, P_{er}, as shown in (20) and (23).

VI. NER SYSTEM

For comparison, the FD relaying system with an EH-enabled source and an ordinary relay without the energy-recycling capability in [19] is analyzed below. The system protocol is illustrated in Fig. 3 where there is no energy recycling at the relay. As a result, different from the proposed SER system which can switch from the fixed power to the self-recycled power and vice versa at the beginning of each phase, in the NER system, the relay must use the fixed power supply P_r during the whole block time T. In the EH phase, the RF signal is sent from the relay to the EH receiver at the source node. In the information transmission phase, the harvested energy at the source is used for transmitting information to the relay and, at the same time, the fixed power supply at the relay is used for transmitting information to the destination.

Recall the equation (1), it is also the received energy signal at S in the NER system. The harvested power at S is P_s as illustrated in (3). The received signal at the destination of the NER system is similar to (19), except that the amplifying factor at R is

$$\xi_n^2 = \frac{P_r}{\frac{|h_{SR}|^2 P_s}{d_1^\beta} + \frac{N_0}{2\rho}}. \tag{29}$$

Thus, the end-to-end SNR and the outage probability as illustrated in [19] are

$$\gamma_n = \frac{\frac{P_r P_s |h_{SR}|^2 |h_{RD}|^2}{d_1^m d_2^m \left(\frac{N_0}{2\rho} + \frac{P_s |h_{SR}|^2}{d_1^m}\right)}}{\frac{N_0 P_r |h_{RD}|^2}{2 d_2^m \rho \left(\frac{N_0}{2\rho} + \frac{P_s |h_{SR}|^2}{d_1^m}\right)} + N_0}, \tag{30}$$

where P_s follows (3). The outage probability, P_n, in the NER system is

$$P_n = \Pr\left\{\frac{a' \gamma_{th} X^2 Y}{b' X^2 + c' Y + d'} < \gamma_{th}\right\}, \tag{31}$$

where

$$\begin{aligned} a' &= 2\eta_1 \alpha \rho P_r^2, \\ b' &= 2\gamma_{th} \rho \eta_1 \alpha P_r d_2^\beta N_0, \end{aligned}$$

$$\begin{aligned} c' &= \gamma_{th} N_0 P_r (d_1^\beta)^2 (1-\alpha), \\ d' &= \gamma_{th} N_0^2 (d_1^\beta)^2 d_2^\beta (1-\alpha). \end{aligned} \tag{32}$$

and $X \triangleq |h_{SR}|^2 |h_{RS}|^2$, $Y \triangleq |h_{RD}|^2$.

The system throughput is computed as [19, Eq. (35)]

$$R_n(\alpha) = R_c(1-\alpha) \int_{b'/a'}^{\infty} u' K_1(u') \frac{1}{\lambda_d} e^{-\frac{z}{\lambda_d}} dz, \tag{33}$$

where

$$u' = 2\sqrt{\frac{c'z + d'}{\lambda_s^2 (a'z - b')}}. \tag{34}$$

The outage probability of the SER system proposed in this paper depends on four random variables, $|h_{SR}|^2$, $|h_{RS}|^2$, $|h_{RD}|^2$, and $|h_{RR}|^2$ where h_{RR} is the channel gain of the loop-back channel at the relay, while that of the NER system in [19] depends on three random variables, $|h_{SR}|^2$, $|h_{RS}|^2$, and $|h_{RD}|^2$. As a result, the derivation of the outage probability and the throughput in the two systems are considerably different. This can be seen clearly from (23), where four variables X_1, X_2, Y, and Z are involved (unlike (31) in the NER system where three variables $|h_{SR}|^2$, $|h_{RS}|^2$, and $|h_{RD}|^2$ are involved). Besides, in (28), the integration is taken over the product of the two modified-Bessel functions of the second kind (rather than the integration of the single modified-Bessel function of the second kind in (33) in the NER system).

VII. NUMERICAL RESULTS

We assume the path loss exponent is $\beta = 3$. Since the efficiency is proportional to the average signal power at the input of the rectifier [20], we assume that the EH efficiency at S is $\eta_1 = 0.4$ and at R is $\eta_2 = 0.8$ (except Fig. 13 where we consider the whole possible range of η_1 and two different values of η_2). The noise power N_0 is assumed to be -90 dBm, and the transmission rate of the source is 8 bits/sec/Hz. The polarization dissimilarity factor is $\rho = 1$, i.e., the polarization states of the desired signal and the SI signal are orthogonal, except Fig. 12 where we consider the whole possible range of ρ. The carrier frequency of 300 MHz is considered and the distance between the Rx antenna of the relay and its Tx antenna is $d_3 = 1$ m to make sure the two antennas experience independent fading. In this paper, we aim to quantify the power saving and the throughput improvement when adopting SER. The protocols of the SER and NER systems are illustrated in Figs. 2 and 3, respectively. For a fair comparison, the EH fraction, α, of the SER and NER systems is set to be the same in each comparison to keep the harvested energy at the source to be the same.

Fig. 4 illustrates the throughput comparison between the proposed FD-SER system $R_c(\alpha)$ (cf. Eq. (28)) and the FD-NER system $R_n(\alpha)$ (cf. Eq. (33)). The notations A.SER and S.SER stand for the analytical results and the simulation results of the SER system, respectively. A.NER represents the analytical results of the non-energy-recycling system in [19]. The results show that the throughput of the proposed FD-SER system almost reaches that of the FD-NER system within the

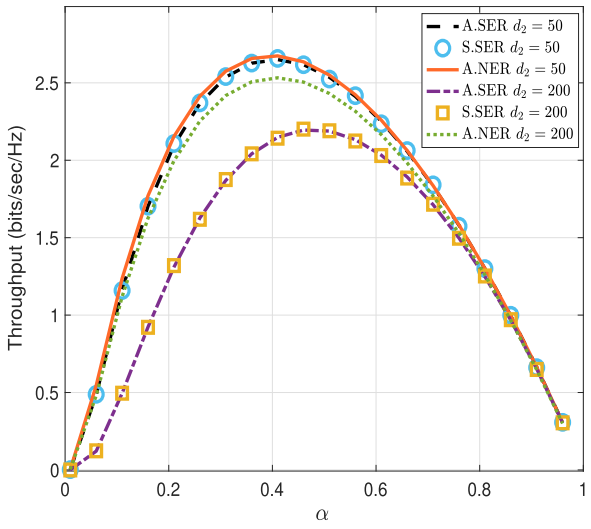

FIGURE 4. Throughput v.s. α when $P_r = 0.1$ Watts and $d_1 = 20$ m.

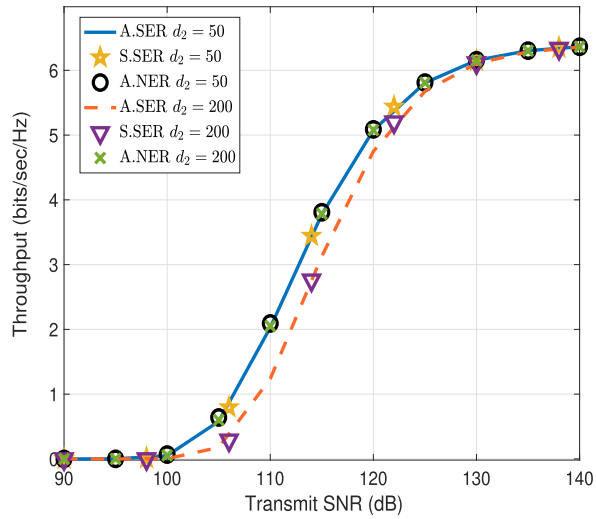

FIGURE 5. Throughput v.s. transmit SNR when $\alpha = 0.2$ and $d_1 = 20$ m.

whole range $0 < \alpha < 1$ when the R-D distance is $d_2 = 50$ m. Recall that the relay only uses the power αP_r in the whole block T in the proposed system, while it uses the power P_r in the FD-NER system. Thus, we define the normalized power consumption as the ratio of the consumed power at the relay of the FD-SER system to that of the FD-NER system, i.e., $\frac{P_c}{P_n} = \frac{\alpha P_r}{P_r} = \alpha$. Note that $0 < \alpha < 1$. This means that the FD-SER system can save the power consumption by $(1-\alpha)P_n$ Watts while having almost the same throughput as the FD-NER one for the small-to-medium R-D distance range (some tens of meters). With the increase of d_2, the throughput of the FD-SER system is getting worse than that of the FD-NER system as expected, because the self-recycled energy at the relay is limited.

Fig. 5 compares the throughputs of the two systems versus the transmit SNR for different R-D distances, d_2. The transmit SNR at the relay is defined as $\frac{P_r}{N_0}$. The throughputs of the

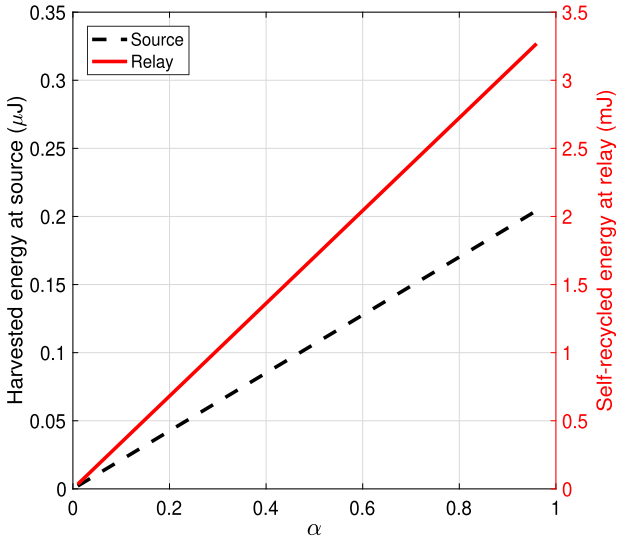

FIGURE 6. Harvested energy v.s. α when $P_r = 1$ Watt and $T = 4.256$ ms.

two systems are almost the same for the whole considered transmit SNR range, if the R-D distance is in a small-to-medium range. For a long-distance range, the throughput of the FD-SER system is slightly worse than that of the FD-NER system unless the transmit SNR is large enough.

Fig. 6 plots the effect of α on the harvested energy at the source node and the self-recycled energy at the relay node in our proposed SER system when $P_r = 1$ Watt and $T = 4.256$ ms [25]. The S-R distance is $d_1 = 20$ m and the distance between the antennas at the relay is $d_3 = 1$ m. The results show that the recycled energy at R is around sixteen thousand times the harvested energy at S due to the influence of path loss and energy conversion efficiencies. The results also reveal that adopting the SER technique at the relay can reuse a significant amount of energy.

Fig. 7 plots the normalized throughput of the FD-SER system $\frac{R_c}{R_n}$ for different values of the normalized power consumption $\frac{P_c}{P_n}$ (a.k.a. α) for $P_r = 1$ Watt. The result shows that, when $P_c = 0.2P_n$, the throughput is $R_c = 0.97R_n$ for $d_2 = 50$ m and $R_c = 0.66R_n$ for $d_2 = 200$ m. This means that the FD-SER system can save 80% of power to achieve 97% of the throughput achieved in the FD-NER counterpart for $d_2 = 50$ m, and 66% of the throughput for $d_2 = 200$ m. The worst point is $P_c = 0.06P_n$ for both $d_2 = 50$ m and $d_2 = 200$ m. At this point, 94% power is saved to have 90% of the throughput achieved in the FD-NER system for $d_2 = 50$ m, and 25% of the throughput for $d_2 = 200$ m. These observations indicate that our FD-SER system can save a large amount of power, while still being able to achieve a relatively high throughput in a small-to-medium R-D distance range.

Fig. 8 illustrates the optimal EH fraction, α, for different relay transmit powers when $d_1 = 20$ m and $d_2 = 50$ m in both the SER and NER systems. Fig. 8 shows that the optimal α decreases with the increase of P_r and the optimal α is almost

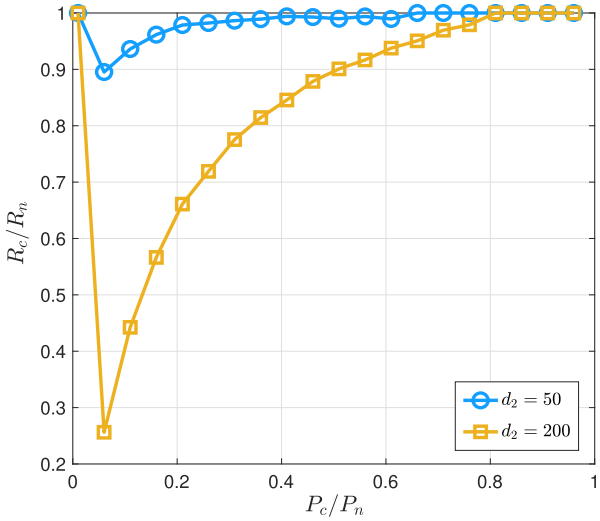

FIGURE 7. Normalized throughput v.s. normalized power consumption when $P_r = 1$ Watt and $d_1 = 20$ m.

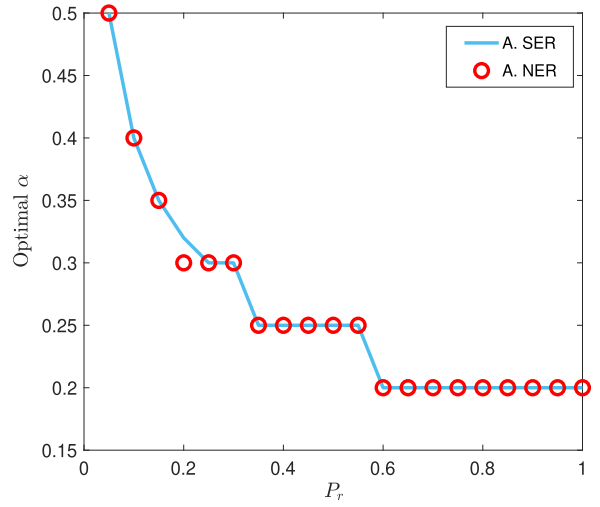

FIGURE 8. Optimal EH fraction v.s. relay transmit power P_r when $d_1 = 20$ m and $d_2 = 50$ m.

the same in these two systems for the considered distances of S-R and R-D.

Fig. 9 illustrates the throughput performance in both the SER and NER systems when $\alpha = 0.4$ and $d_1 = 20$ m. In this figure, P_r is selected as 0.25 Watts and 0.1 Watts for the SER and NER systems, respectively, to guarantee the same total consumed power in the two system for a fair comparison. Recall Figs. 4 and 8, it is clear that $\alpha = 0.4$ will optimize the throughput of the NER system for a wide range of d_2 from 50 m to 200 m when $P_r = 0.1$ Watts. However, $\alpha = 0.4$ is not the optimal value of the SER system when $P_r = 0.25$ Watts. This means Fig. 9 compares the throughput of the SER system with the optimal throughput of the NER one, given that the total power consumption of the two systems is the same. Thus, this figure shows the minimum throughput improvement that could be achieved by the proposed SER system,

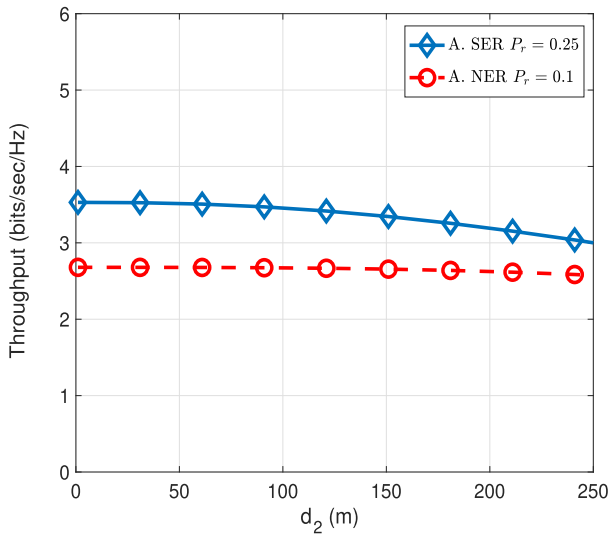

FIGURE 9. Throughput v.s. the R-D distance d_2 when $\alpha = 0.4$ and $d_1 = 20$ m.

compared to the NER counterpart, for the considered set of parameters.

Fig. 10 examines the impact of the distance d_2 and the transmit power at the relay, P_r, on the throughput of the FD-SER and FD-NER systems. Our analyses are derived for generic α values. As we need to make sure that α is the same in both the SER and NER systems for a fair comparison, the parameter $\alpha = 0.2$ is chosen in both system as an example for illustration. Besides, the EH fraction α is set to be 0.2 as it is the optimal value for $P_r = 1$ Watt as shown in Fig. 8. Thus, the following figures (Figs. 10-13) show the upper bound of the throughput improvement that could be achieved by the SER system, compared to the NER counterpart. Fig. 10a compares the throughput of the SER and NER systems when the same transmit power is used at the relay and $\alpha = 0.2$ in both systems. From Fig. 10a, the throughputs of these two systems are almost the same when d_2 is less than 90 m for $P_r = 1$ Watt and when d_2 is less than 50 m for $P_r = 0.1$ Watts. These observations prove that the consumed power in the proposed system is reduced by 80% to achieve the same throughput compared to the non-recycling system for a small-to-medium range of d_2. Fig. 10b shows that the throughput of the FD-SER system is 5.08 bits/sec/Hz when $d_2 = 20$ m and 4.75 bits/sec/Hz when $d_2 = 200$ m. Meanwhile, the throughput of the FD-NER system reduces slowly from 3.15 bits/sec/Hz at $d_2 = 20$ m to 3.12 bits/sec/Hz at $d_2 = 200$ m. Note that the power consumed at the relay of the proposed FD-SER system is 0.2 Watts when $\alpha = 0.2$ and $P_r = 1$ Watts, which is exactly the same as the power consumed at the relay of the FD-NER system with $P_r = 0.2$ Watts. This result shows that, with the same consumed power, the throughput in our FD-SER system can be up to 1.61 times higher than that in the FD-NER system. This is because the FD-SER system saves the energy consumed in

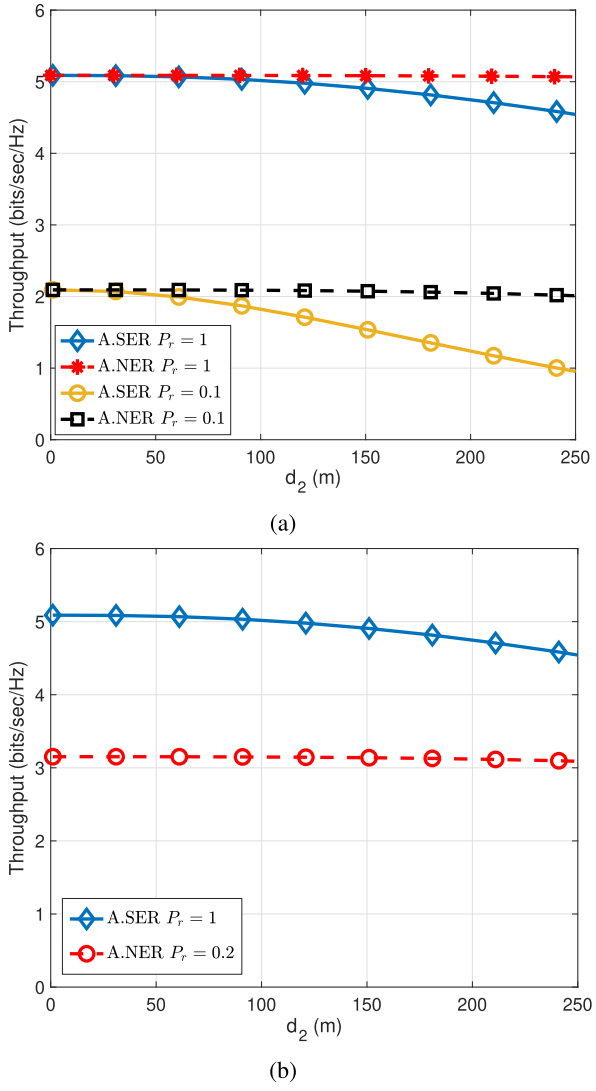

FIGURE 10. Throughput v.s. the R-D distance d_2 when $\alpha = 0.2$ and $d_1 = 20$ m.

the second phase by adopting the SER technique. The relay in the FD-SER system uses a higher power, compared to the FD-NER one, to transmit energy signals to the source and itself in the first phase. Thus, the FD-SER system boosts the system throughput by 1.61 times the FD-NER system with the same power consumption.

Fig. 11 plots the throughput performance of the proposed FD-SER system versus the Source-Relay (S-R) distance d_1 when $\alpha = 0.2$, with the non-cycling system serving as a benchmark. As mentioned above, the relay-transmitting power in the second phase of the FD-SER system depends on the harvested energy while the FD-NER system relay has the fix power supply. When $\alpha = 0.2$ and $P_r = 1$ Watts, the total consumed power of the FD-SER system is exactly the same as that of the FD-NER system with $P_r = 0.2$ Watts. The total Source-Destination (S-D) distance is set to be 200 m and the S-R distance is $d_2 = 200 - d_1$ m. Fig. 11 aims to explore the effect of relay location on the system throughput

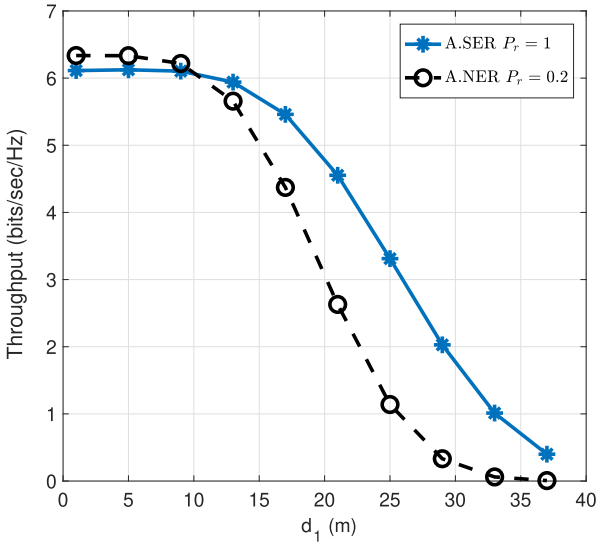

FIGURE 11. Throughput v.s. d_1 when $\alpha = 0.2$ and $d_2 = 200 - d_1$ m.

in comparison with the NER counterpart. As a result, the same total S-D distance of 200 m is considered in both systems. The results show that the throughput in both systems decreases as d_1 increases due to a larger path loss in the S-R link. Consequently, the received signal strength at the relay is poorer and the throughput decreases. However, the proposed system still outperforms the FD-NER system, unless d_1 is under 10 m, where the former is slightly inferior than the latter. This is because, when d_1 is too small, the relay is too far from the destination. Due to the limited recycled energy at the relay, the system throughput will be reduced. Fig. 11 thus shows the trade-off between the two systems. For this simulation scenario, if the relay has to be put more than 10 m away from the source due to, for example, the unavailability of the physical place for the installation of the relay (like in mining tunnels), the proposed FD-SER system is a better choice than the counterpart. This demonstrates the usefulness of our proposed system in a realistic scenario. Clearly, the optimal relay location in the proposed system is approaching the source node, rather than the middle point between the source and the destination which is a well-known observation for a conventional half-duplex, non-energy harvesting system reported in the literature.

Fig. 12 plots the throughput of the FD-SER and FD-NER systems versus the polarization dissimilarity factor, ρ, when $\alpha = 0.2$. The comparison of the two systems is based on the same total energy consumption, so $P_r = 1$ in the SER system and $P_r = 0.2$ in the SER system. The analytical results show that the throughput increases with the increase of ρ. Since $0 < \rho \leqslant 1$, the maximum throughput is obtained when $\rho = 1$, i.e., the polarization states of the desired signal and the SI signal are orthogonal. Fig. 12 indicates clearly that our proposed system still outperforms the FD-NER one even when the polarization states of the antennas are not orthogonal.

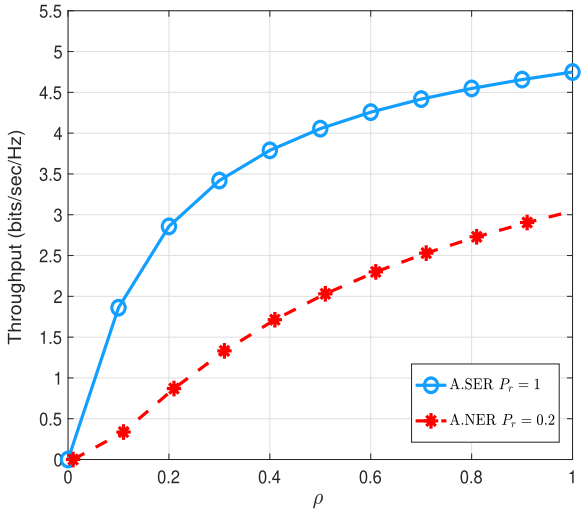

FIGURE 12. Throughput v.s. polarization dissimilarity factor, ρ, when $\alpha = 0.2$.

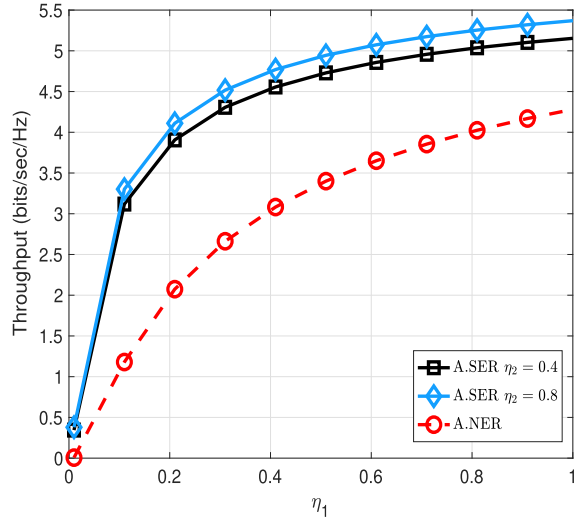

FIGURE 13. Throughput v.s. efficiency at S, η_1, when $P_r = 1$ Watt in the FD-SER system and $P_r = 0.2$ Watts in the FD-NER system.

Fig. 13 illustrates the impact of the energy efficiency at S, η_1, on the system throughput. We set $\alpha = 0.2$, $d_1 = 20$ m, $d_2 = 200$ m, and $P_r = 1$ Watt in the FD-SER system and $P_r = 0.2$ Watts in the FD-NER system. Note that usually $\eta_2 > \eta_1$ as the distance between the transmit-end and the receive-end of the energy signal at R is closer than that at S. Fig. 13 reveals that throughput is proportional to η_1 in both systems. The increase of the efficiency at R, η_2, in the FD-SER system will improve further the system throughput. In addition, if η_1 increases by 0.4, the throughput increases by about 0.4 bits/sec/Hz to 4.8 bits/sec/Hz. This figure also shows the variation of η_2 in terms of $\eta_2 = 0.4$ and $\eta_2 = 0.8$. If η_2 increases by 0.4, the throughput increases by about 0.2 bits/sec/Hz. Thus, it is clear that the throughput depends more on η_1 rather than η_2.

VIII. CONCLUSION

In this paper, we have proposed a Polarization-Enabled Digital Self-Interference Cancellation (PDC)-based FD relaying network with an EH-enabled source and a SER-enabled relay. The relay only uses its fixed power supply in the first phase to broadcast energy signals to the sources. During this process, it also recycles part of its own transmitted energy. In the remaining phase, the relay uses the recycled power to forward signals from the source to the destination in a PDC-based FD communication mode. Analytical expressions have been derived for the outage probability and throughput of the system, confirmed by our simulations. The paper reveals that, compared to the FD-NER system, our proposed system can save significantly the total consumed power while achieving almost the same system throughput for a small-to-medium R-D distance range. Alternatively, with the same power consumption, our system outperforms the counterpart in most cases. Therefore, it is a promising solution to save power or boost the system throughput in FD EH relaying systems. Our future works include extending the two-antenna relay to a multi-antenna structure, considering other SIC techniques, such as the analog least mean square loop [26], and examining the correlated fading channels between antennas [27].

REFERENCES

[1] Z. Wei, X. Zhu, S. Sun, Y. Jiang, A. Al-Tahmeesschi, and M. Yue, "Research issues, challenges, and opportunities of wireless power transfer-aided full-duplex relay systems," *IEEE Access*, vol. 6, pp. 8870–8881, 2018.

[2] J. Li, L. C. Tran, and F. Safaei, "Outage probability and throughput analyses in full-duplex relaying systems with energy transfer," *IEEE Access*, vol. 8, pp. 150150–150161, 2020.

[3] V.-D. Nguyen, T. Q. Duong, H. D. Tuan, O.-S. Shin, and H. V. Poor, "Spectral and energy efficiencies in full-duplex wireless information and power transfer," *IEEE Trans. Commun.*, vol. 65, no. 5, pp. 2220–2233, May 2017.

[4] K. Kwon, D. Hwang, H.-K. Song, and S. S. Nam, "Full-duplex with self-energy recycling in the RF powered multi-antenna relay channels," *IEEE Signal Process. Lett.*, vol. 26, no. 10, pp. 1516–1520, Oct. 2019.

[5] Y. Zeng and R. Zhang, "Full-duplex wireless-powered relay with self-energy recycling," *IEEE Wireless Commun. Lett.*, vol. 4, no. 2, pp. 201–204, Apr. 2015.

[6] O. T. Demir and T. E. Tuncer, "Optimum QoS-aware beamformer design for full-duplex relay with self-energy recycling," *IEEE Wireless Commun. Lett.*, vol. 7, no. 1, pp. 122–125, Feb. 2018.

[7] S. Xu, X. Song, Z. Xie, J. Cao, and J. Wang, "Secrecy transmission for self-energy recycling untrusted relay networks with imperfect channel state information," *IEEE Access*, vol. 7, pp. 169724–169733, 2019.

[8] D. Hwang, K. C. Hwang, D. I. Kim, and T.-J. Lee, "Self-energy recycling for RF powered multi-antenna relay channels," *IEEE Trans. Wireless Commun.*, vol. 16, no. 2, pp. 812–824, Feb. 2017.

[9] J. Qiao, H. Zhang, F. Zhao, and D. Yuan, "Secure transmission and self-energy recycling with partial eavesdropper CSI," *IEEE J. Sel. Areas Commun.*, vol. 36, no. 7, pp. 1531–1543, Jul. 2018.

[10] Z. Wang, X. Yue, and Z. Peng, "Full-duplex user relaying for noma system with self-energy recycling," *IEEE Access*, vol. 6, pp. 67057–67069, 2018.

[11] L. Zhang, Y. Cai, M. Zhao, B. Champagne, and L. Hanzo, "Nonlinear MIMO transceivers improve wireless-powered and self-interference-aided relaying," *IEEE Trans. Wireless Commun.*, vol. 16, no. 10, pp. 6953–6966, Oct. 2017.

[12] S. Yang, Y. Ren, G. Lu, and J. Wang, "Optimal resource allocation for full-duplex wireless-powered relaying with self-energy recycling," in *Proc. 11th Int. Conf. Wireless Commun. Signal Process. (WCSP)*, Xi'an, China, Oct. 2019, pp. 1–6.

[13] Ö. T. Demir and T. E. Tuncer, "Robust optimum and near-optimum beamformers for decode-and-forward full-duplex multi-antenna relay with self-energy recycling," *IEEE Trans. Wireless Commun.*, vol. 18, no. 3, pp. 1566–1580, Mar. 2019.
[14] H. Liu, K. J. Kim, K. S. Kwak, and H. V. Poor, "Power splitting-based SWIPT with decode-and-forward full-duplex relaying," *IEEE Trans. Wireless Commun.*, vol. 15, no. 11, pp. 7561–7577, Nov. 2016.
[15] M. H. N. Shaikh, V. A. Bohara, and A. Srivastava, "Performance analysis of a full-duplex MIMO decode-and-forward relay system with self-energy recycling," *IEEE Access*, vol. 8, pp. 226248–226266, 2020.
[16] A. El Shafie and N. Al-Dhahir, "Secure communications in the presence of a buffer-aided wireless-powered relay with self-energy recycling," *IEEE Wireless Commun. Lett.*, vol. 5, no. 1, pp. 32–35, Feb. 2016.
[17] X. Zhou, R. Zhang, and C. K. Ho, "Wireless information and power transfer: Architecture design and rate-energy tradeoff," *IEEE Trans. Commun.*, vol. 61, no. 11, pp. 4754–4767, Nov. 2013.
[18] C. C. Y. Poon, B. P. L. Lo, M. R. Yuce, A. Alomainy, and Y. Hao, "Body sensor networks: In the era of big data and beyond," *IEEE Rev. Biomed. Eng.*, vol. 8, pp. 4–16, 2015.
[19] J. Li, L. C. Tran, and F. Safaei, "Throughput analysis of in-band full-duplex transmission networks with wireless energy harvesting enabled sources," *IEEE Access*, vol. 9, pp. 74989–75002, 2021.
[20] B. Clerckx, R. Zhang, R. Schober, D. W. K. Ng, D. I. Kim, and H. V. Poor, "Fundamentals of wireless information and power transfer: From RF energy harvester models to signal and system designs," *IEEE J. Sel. Areas Commun.*, vol. 37, no. 1, pp. 4–33, Jan. 2019.
[21] E. Boshkovska, D. W. K. Ng, N. Zlatanov, and R. Schober, "Practical non-linear energy harvesting model and resource allocation for SWIPT systems," *IEEE Commun. Lett.*, vol. 19, no. 12, pp. 2082–2085, Dec. 2015.
[22] R. T. Behrens and L. L. Scharf, "Signal processing applications of oblique projection operators," *IEEE Trans. Signal Process.*, vol. 42, no. 6, pp. 1413–1424, Jun. 1994.
[23] I. S. Gradshteyn and I. M. Ryzhik, *Table of Integrals, Series, and Products*, 5th ed. New York, NY, USA: Academic, 1996.
[24] C. Zhong, H. A. Suraweera, G. Zheng, I. Krikidis, and Z. Zhang, "Wireless information and power transfer with full duplex relaying," *IEEE Trans. Commun.*, vol. 62, no. 10, pp. 3447–3461, Oct. 2014.
[25] B. Varghese, N. E. John, S. Sreelal, and K. Gopal, "Design and development of an RF energy harvesting wireless sensor node (EH-WSN) for aerospace applications," *Proc. Comput. Sci.*, vol. 93, pp. 230–237, Jan. 2016.
[26] A. T. Le, L. C. Tran, X. Huang, Y. J. Guo, and J. Y. C. Vardaxoglou, "Frequency-domain characterization and performance bounds of ALMS loop for RF self-interference cancellation," *IEEE Trans. Commun.*, vol. 67, no. 1, pp. 682–692, Jan. 2019.
[27] L. C. Tran, T. A. Wysocki, A. Mertins, and J. Seberry, "A generalized algorithm for the generation of correlated Rayleigh fading envelopes in wireless channels," *EURASIP J. Wireless Commun. Netw.*, vol. 2005, no. 5, pp. 801–815, Dec. 2005.

JIAMAN LI received the B.E. degree (Hons.) from the University of Wollongong, Australia, and Zhengzhou University, China, in 2016. She is currently pursuing the Ph.D. degree with the University of Wollongong. Her current research interests include full-duplex communications in energy harvesting relaying networks.

LE CHUNG TRAN (Senior Member, IEEE) received the B.E. degree (Hons.) from the University of Transport and Communications (UTC), in 1997, the M.E. degree (Hons.) from the University of Science and Technology, Vietnam, in 2000, and the Ph.D. degree from the University of Wollongong (UOW), Australia, in 2006, all in telecommunications engineering. He was a Lecturer with UTC, from 1997 to 2012. From 2005 to 2006, he was an Associate Research Fellow with the Wireless Technologies Laboratory, UOW. From 2006 to 2008, he was a Postdoctoral Research Fellow with the University of Lübeck, Germany, under the Alexander von Humboldt (AvH) Fellowship. He has been with UOW, since 2009, where he is currently a Senior Lecturer. He has coauthored 100 publications, including the Springer book *Complex Orthogonal Space-Time Processing in Wireless Communications*, which is hold in 354 worldwide libraries. His research interests include 5G, MIMO, WBANs, positioning, navigation, and digital signal processing for communications. He has achieved the World University Services (WUS) awards (twice), the Vietnamese Government's Doctoral Scholarship, the International Postgraduate Research Scholarship (IPRS), the prestigious Humboldt fellowships (twice), and the University Outstanding Contribution to Teaching and Learning (2019-OCTAL) Award. He has served as an Organizing Committee Member (the Track Chair, the Session Chair, and the Publicity Co-Chair), a Technical Program Committee (TPC) member for over 30 IEEE conferences, and a Keynote Speaker for IEEE ICSPCS2019 Conference. He has served as an Associate Editor for *IET Wireless Sensor Systems*, an Advisory Board Member for Cambridge Scholars Publishing, and an Editorial Board Member of the *Electrical Engineering: An International Journal* (EEIJ).

FARZAD SAFAEI (Senior Member, IEEE) received the B.Eng. (electronics) degree from The University of Western Australia and the Ph.D. degree in telecommunications engineering from Monash University, in 1998. He is currently the Chair of telecommunications engineering at the University of Wollongong. Before joining the University of Wollongong, he was the Manager of the Internetworking Architecture and Services Section, Telstra Research Laboratories. He was the Managing Director of the ICT Research Institute, from 2008 to 2013, and the Program Director of the Smart Services Cooperative Research Centre, Australia, from 2007 to 2014. His main research interests include multimedia signal processing and communications technology. He is the Winner of a number of awards, including the top Australian and Asia Pacific Awards for ICT Research and Development, in 2012.